0026-895X/05/6704-1268–1282$20.00
MOLECULAR PHARMACOLOGY
Vol. 67, No. 4
8565/1197984
Mol Pharmacol 67:1268–1282, 2005
Printed in U.S.A.

The CCR5 Receptor-Based Mechanism of Action of 873140, a Potent Allosteric Noncompetitive HIV Entry Inhibitor[S]

Christian Watson, Stephen Jenkinson, Wieslaw Kazmierski, and Terry Kenakin

Assay Development and Compound Profiling (C.W., T.K.), Departments of Biochemical and Analytical Pharmacology (S.J.) and Medicinal Chemistry (W.K.), GlaxoSmithKline Research and Development, Research Triangle Park, North Carolina

Received October 21, 2004; accepted January 10, 2005

ABSTRACT

4-{[4-({(3*R*)-1-Butyl-3-[(R)-cyclohexyl(hydroxy)methyl]-2,5dioxo-1,4,9-triazaspiro[5.5]undec-9-yl}methyl)phenyl]oxy}benzoic acid hydrochloride (873140) is a potent noncompetitive allosteric antagonist of the CCR5 receptor ($pK_B = 8.6 \pm 0.07$; 95% CI, 8.5 to 8.8) with concomitantly potent antiviral effects for HIV-1. In this article, the receptor-based mechanism of action of 873140 is compared with four other noncompetitive allosteric antagonists of CCR5. Although (*Z*)-(4-bromophenyl){1′-[(2,4-dimethyl-1-oxido-3-pyridinyl)carbonyl]-4′-methyl-1,4′-bipiperidin-4-yl}methanone *O*-ethyloxime (Sch-C ; SCH 351125), 4,6-dimethyl-5-{[4-methyl-4-((3*S*)-3-methyl-4-{(1*R*)-2-(methyloxy)-1-[4-(trifluoromethyl)phenyl]ethyl}-1-piperazinyl)-1-piperidinyl]carbonyl}pyrimidine (Sch-D; SCH 417,690), 4,4-difluoro-*N*-((1*S*)-3-{(3-*endo*)-3-[3-methyl-5-(1-methylethyl)-4*H*-1,2,4-triazol-4-yl]-8-azabicyclo[3.2.1]oct-8-yl}-1-phenylpropyl)cyclohexanecarboxamide (UK-427,857), and *N*,*N*-dimethyl-*N*-[4-[[[2-(4-methylphenyl)-6,7-dihydro-5*H*-benzocyclohepten-8-yl]carbonyl]amino]benzyl]tetrahydro-2*H*-pyran-4-aminium chloride (TAK779) blocked the binding of both chemokines ^{125}I-MIP-1α (also known as ^{125}I-CCL3, ^{125}I-LD78) and ^{125}I-RANTES (^{125}I-CCL5), 873140 was an ineffectual antagonist of ^{125}I-RANTES (regulated on activation normal T cell expressed and secreted) binding (but did block binding of ^{125}I-MIP-1α). Furthermore, 873140 blocked the calcium response effects of CCR5 activation by CCL5 (RANTES) (as did the other antagonists), indicating a unique divergence of blockade of function and binding with this antagonist. The antagonism of CCR5 by 873140 is saturable and probe-dependent, consistent with an allosteric mechanism of action. The blockade of CCR5 by 873140 was extremely persistent with a rate constant for reversal of <0.004 h^{-1} ($t_{1/2} > 136$ h). Coadministration studies of 873140 with the four other allosteric antagonists yielded data that are consistent with the notion that all five of these antagonists bind to a common allosteric site on the CCR5 receptor. Although these ligands may have a common binding site, they do not exert the same allosteric effect on the receptor, as indicated by their differential effects on the binding of ^{125}I-RANTES. This idea is discussed in terms of using these drugs sequentially to overcome HIV viral resistance in the clinic.

With the discovery that the R5 strain of HIV uses the chemokine C CCR5 receptor for cell infection (Alkhatib et al., 1996; Choe et al., 1996; Doranz et al., 1996; Dragic et al., 1996; Deng et al., 1997; Shieh et al., 1998; Zhang and Moore, 1999) has come the opportunity for a completely new approach to preventing HIV infection: blockade of CCR5 receptor interaction with the viral coat protein gp120. Subsequent reports of potent antagonists of CCR5-mediated HIV entry (Baba et al., 1999; Finke et al., 2001; Strizki et al., 2001; Kazmierski et al., 2003; Demarest et al., 2004a,b, Maeda et al., 2004) have validated this approach and have possibly opened a new era of AIDS therapy. There are data to support the notion that an allosteric mechanism is involved in the antagonism of HIV by low molecular weight antagonists of CCR5 (Kazmierski et al., 2002). The large size of the proteins involved in HIV fusion (i.e., CCR5 and gp120) and the fact that mutational studies indicate that numerous regions of both CCR5 (Atchison et al., 1996; Rucker et al., 1996; Doms and Peiper, 1997; Doranz et al., 1997; Picard et al., 1997; Lee

[S] The online version of this article (available at http://molpharm.aspetjournals.org) contains supplemental material.

Article, publication date, and citation information can be found at http://molpharm.aspetjournals.org.
doi:10.1124/mol.104.008565.

ABBREVIATIONS: MIP-1α, macrophage inflammatory protein 1-alpha (standard nomenclature CCL3, also known as LD78); CHO, Chinese hamster ovary; SPA, scintillation proximity assay; DMSO, dimethyl sulfoxide; RT, room temperature; HEK, human embryonic kidney; FLIPR, fluorometric imaging plate reader; RANTES, regulated on activation, normal T cell expressed and secreted (standard nomenclature for this chemokine is CCL5); Sch-C (SCH 351125), (*Z*)-(4-bromophenyl){1′-[(2,4-dimethyl-1-oxido-3-pyridinyl)carbonyl]-4′-methyl-1,4′-bipiperidin-4-yl}methanone *O*-ethyloxime; Sch-D (SCH 417,690), 4,6-dimethyl-5-{[4-methyl-4-((3*S*)-3-methyl-4-{(1*R*)-2-(methyloxy)-1-[4-(trifluoromethyl)phenyl-]ethyl}-1-piperazinyl)-1-piperidinyl]carbonyl}pyrimidine; UK-427,857, 4,4-difluoro-*N*-((1*S*)-3-{(3-*endo*)-3-[3-methyl-5-(1-methylethyl)-4*H*-1,2,4-triazol-4-yl]-8-azabicyclo[3.2.1]oct-8-yl}-1-phenylpropyl)cyclohexanecarboxamide; TAK779, *N*,*N*-dimethyl-*N*-[4-[[[2-(4-methylphenyl)-6,7-dihydro-5*H*-benzocyclohepten-8-yl]carbonyl]amino]benzyl]tetrahydro-2*H*-pyran-4-aminium chloride; UCB35625, 1-Cycloheptylmethyl-4-{[1-(2,7-dichloro-9*H*-xanthen-9-yl)-methanoyl]-amino}-1-methyl-piperidinium; CI, confidence interval.

et al., 1999) and gp120 (Bieniasz et al., 1997; Kwong et al., 1998; Rizzuto et al., 1998; Smyth et al., 1998; Ross et al., 1999) interact to promote HIV infection suggest that low molecular weight antagonists of CCR5 preventing this process act through an allosteric mechanism (Kazmierski et al., 2002). In fact, an allosteric interaction between the HIV-1 envelope glycoprotein and the anti-HIV chemokine MIP-1β has been directly shown with kinetic binding studies (Staudinger et al., 2001). Consistent with this idea are data to indicate that there are separate binding loci on CCR5 for small antagonists such as Sch-C and the peptide chemokine RANTES (Wu et al., 1997; Blanpain et al., 2003; Tsamis et al., 2003). This present article explores the mechanism of blockade of CCR5 receptors by a new potent antiviral 873140 (Demarest et al., 2004a,b; Maeda et al., 2004) and other CCR5 antagonists (see Fig. 1) and the relationship of this mechanism to therapeutic use and viral resistance.

Materials and Methods

CCR5 CHO Membrane Preparation. Chinese hamster ovary (CHO) cells stably expressing the human CCR5 receptor were grown in suspension with media containing 95% Excel 301, 5% fetal bovine serum, 4 mM L-glutamine, and 250 μg/ml G418 (Invitrogen, Carlsbad, CA), harvested, and pelleted by centrifugation. The weighed pellet was homogenized in 5 volumes of ice-cold buffer containing 50 mM HEPES (Invitrogen) with protease inhibitor cocktail (2.5 μg/ml Pefabloc, 0.1 μg/ml pepstatin A, 0.1 μg/ml leupeptin, and 0.1 μg/ml aprotinin; Sigma-Aldrich, St. Louis, MO) at pH 7.4. The mixture was re-homogenized with a glass Dounce homogenizer for 10 to 20 strokes. Homogenate was centrifuged at 18,000 rpm in a F28/36 rotor using a Sorvall RC26. The supernatant was discarded and pellet resuspended in 3 volumes of HEPES buffer. The pellet was homogenized and resuspended a total of three times. Finally, the pellet was reweighed, homogenized in 3× weight-to-volume HEPES buffer, and aliquoted in 0.5- to 1.5-ml volumes into small vials for storage at −80°C. The protein concentration was determined using a BCA kit (Pierce, Rockford, IL).

SPA Binding Studies. CHO cells stably expressing the human CCR5 receptor were cultured in suspension and scaled up, and membranes generated by a standard membrane preparation protocol. Ligand binding to CCR5 CHO membranes was measured using scintillation proximity assay (SPA). All test compounds were serially diluted in 100% DMSO at 100× the final assay concentration. CCR5 receptor membranes (15 μg/well) and WGA SPA beads (250 μg/well; Amersham Biosciences, Piscataway, NJ) were diluted in assay buffer containing 50 mM HEPES, pH 7.4 (Invitrogen), 1 mM $CaCl_2$, 5 mM $MgCl_2$, 1% bovine serum albumin, 0.25 mg/ml bacitracin, 2.5 μg/ml Pefabloc, 0.1 μg/ml Pepstatin A, 0.1 μg/ml leupeptin, 0.1 μg/ml aprotinin, and DMSO added to equal a final concentration of 2% per well (v/v) including compound(s) (all buffer items from Sigma-Aldrich). The receptor/bead slurry was mixed in a 50-ml conical tube and preincubated for 1 h at 4°C to allow the receptor/bead complex to form. After preincubation, each well of a 96-well microtiter plate (Optiplate 96; PerkinElmer Life and Analytical Sciences, Boston, MA) received 1 μl of test compound in 100% DMSO [final concentration, 2% DMSO (v/v)] or appropriate control, 50 μl of receptor/bead mixture and 50 μl of ^{125}I-MIP1α or ^{125}I-RANTES (PerkinElmer Life and Analytical Sciences). Radioligand concentrations were typically 0.17 nM (60,000 cpm) for ^{125}I-MIP1α and 0.05 nM (18,000 cpm) for ^{125}I-RANTES unless otherwise noted. Plates were shaken at RT for 4 h and binding signal was quantified on a TopCount scintillation counter (30 s read) (PerkinElmer Life and Analytical Sciences).

Data reduction was performed using the Microsoft Excel (Microsoft, Redmond, WA) add-ins Robofit or Robosage (GlaxoSmithKline internal package). For concentration-response assays, the result of each test well was expressed as %B/Bo (% total specific binding); curves were generated by plotting the %B/Bo versus the concentration and the IC_{50} derived using the equation

$$Y = V_{max}(1 - ([B]^n/([B]^n + IC_{50}{}^n)) \quad (1)$$

where K_B is the equilibrium dissociation constant of the (antagonist) ligand-receptor complex, V_{max} is the maximal degree of radioligand binding inhibition, and IC_{50} is the molar concentration of antagonist that blocks the binding by 50%. Plates were run for 14-point concentration-response curves in triplicate.

Receptor Occupancy Offset Studies. Offset experiments were run in 1.5-ml microcentrifuge tubes. Receptor/bead mixture (100 μl) was added to all assay tubes. Test compounds were introduced to each tube (1 μl) at the appropriate time points (200× final concentration needed in 100% DMSO) and allowed to incubate at RT for 5 h. Tubes were washed by centrifugation (1000 rpm, 5 min) and supernatant was aspirated. Fresh assay buffer (100 μl) was then added back to each tube. All tubes received equal washes either before or after compound addition to control for potential loss of signal caused by repeated washing. Tubes were stored at 4°C overnight to maintain receptor integrity over the long experimental timeline. Once washes were complete, 50 μl of the compound/receptor/bead mixture from each tube was added to a 96-well microtiter plate. Reaction was initiated with the addition of 50 μl of 1.5 or 0.2 nM ^{125}I-MIP1α. Plates were shaken for 2 h at RT, and binding signal was quantified on a TopCount scintillation counter (30 s read).

BacMam Baculovirus Generation. Recombinant BacMam baculoviruses for CCR5 (GenBank accession no. X91492) and the chimeric G-protein Gqi5 (Conklin et al., 1993) were constructed from pFASTBacMam shuttle plasmids using the bacterial cell-based Bac-to-Bac system (Invitrogen) (Luckow et al., 1993). Viruses were propagated in Sf9 (*Spodoptera frugiperda*) cells cultured in Hink's TNM-FH insect media (JRH Biosciences, Lenexa, KS) supplemented with 10% fetal calf serum (Hyclone, Ogden, UT) and 0.1% (v/v) Pluronic F-68 (Invitrogen) according to established protocols (O'Reilly et al., 1992).

Cell Culture. HEK-293 cells, stably transfected to express the human macrophage scavenging receptor (Class A, Type1; GenBank accession no. D90187), were maintained in Dulbecco's modified Eagle's medium/Ham's F-12 media (1:1 mix) supplemented with 10% heat-inactivated fetal calf serum and 1.5 μg/ml puromycin. The expression of this protein by the HEK-293 cells enhances their ability to stick to tissue culture-treated plasticware. All media, serum and supplements were from Invitrogen.

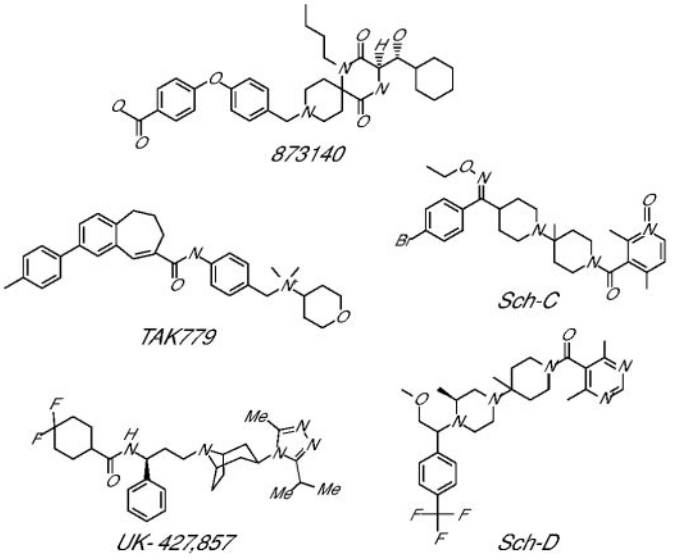

Fig. 1. Chemical structures of CCR5 receptor antagonists.

Transduction of HEK-293 Cells. HEK-293 cells were harvested using a nonenzymatic cell dissociation buffer (Invitrogen) and were subsequently resuspended in culture media supplemented with CCR5 and Gqi5 BacMam viruses (multiplicity of infection of 50 and 12.5, respectively). The cells were plated at a density of 40,000 cells (100 μl volume) per well in black, clear-bottomed, 96-well plates. The plates were incubated at 37°C, 5% CO_2, 95% humidity for 24 h to allow time for CCR5 and Gqi5 protein expression.

Calcium Mobilization Experiments. Growth media was removed from the transduced HEK-293 cells, and they were washed once with FLIPR buffer [Calcium Plus assay kit dye reagent (Molecular Devices, Sunnyvale, CA) dissolved in Dulbecco's modified Eagle's medium/Ham's F-12 media containing 2.5 mM probenicid and 0.1% bovine serum albumin (w/v)]. Fifty microliters of this dye solution was then added to each well and the plates were incubated for 1 h at 37°C, under 5% CO_2 and 95% humidity. The effects of various ligands on intracellular calcium levels were examined using FLIPR (Molecular Devices, Sunnyvale, CA).

Statistical Analysis of Significance of Regression. The relationship between variables was quantified by a t-value calculated as

$$t = r \times \sqrt{\frac{(n-2)}{(1-r^2)}},\ \mathrm{df} = n-2 \tag{2}$$

where

$$r = \frac{s_{xy}}{\sqrt{s^2_x s^2_y}} \tag{3}$$

and

$$s_{xy} = \Sigma \mathrm{xy_i} - \frac{(\Sigma x_i)(\Sigma y_i)}{n_i} \tag{4}$$

$$s^2_x = \Sigma x^2_i - \frac{(\Sigma x)^2}{n_i} \tag{5}$$

and

$$s^2_y = \Sigma y^2_i - \frac{(\Sigma y)^2}{n_i} \tag{6}$$

Kinetics of Offset. Data were fit to a first-order receptor offset model of the form

$$\rho_t = \rho_e e^{-kt} \tag{7}$$

where ρ_e is the fractional receptor occupancy by the antagonist at equilibrium, k is the rate of offset, t is time, and ρ_t is the fractional antagonist receptor occupancy at time t. The values for ρ_e and ρ_t were obtained from mass action:

$$\rho = \frac{[B]/K_B}{[B]/K_B + 1} \tag{8}$$

where $[B]$ is the antagonist concentration and K_B the equilibrium dissociation constant of the antagonist-receptor complex. Values of $[B_e]/K_B$ and $[B_t]/K_B$ were obtained by fitting the values for radioligand binding in the absence and presence of the antagonist to the ^{125}I-MIP-1α saturation curve to the model for simple competitive antagonism for MIP-1α:

$$\rho = \frac{[^{125}\text{I-MIP-1}\alpha/K_d]B_{max}}{[^{125}\text{I-MIP-1}\alpha/K_d] + [B]/K_B + 1} \tag{9}$$

and for noncompetitive antagonists:

$$\rho = \frac{[^{125}\text{I-MIP-1}\alpha/K_d]B_{max}}{[^{125}\text{I-MIP-1}\alpha/K_d]([B]/K_B + 1) + [B]/K_B + 1} \tag{10}$$

A regression of ln (ρ_t/ρ_e) versus time yields a straight line of slope = $-k$.

Drugs and Materials. HEPES (1 M, pH 7.4) was from Invitrogen; bacitracin, bovine serum albumin, $CaCl_2$, and Sigmacote were from Sigma, $MgCl_2$ was from J. T. Baker (Phillipsburg, NJ); MIP1α was from PeproTech (Rocky Hill, NJ); scintillation proximity beads and wheat germ agglutinin were from Amersham Biosciences; ^{125}I-MIP-1α, TOPSEAL-S, and 96-well flat-bottomed Optiplates were from PerkinElmer Life and Analytical Sciences; Falcon 96-well round-bottomed plates were from BD Biosciences Discovery Labware (Bedford, MA); DMSO was from EM Science (Gibbstown, NJ); siliconized pipette tips, volume 200-1300 μl were from Accutip and siliconized pipette tips, volume 1–200 μl were from Bio Plas, Inc. (San Rafael, CA); and reagent reservoir was from ELKay Laboratory Consumables (Shrewsbury, MA).

RANTES and MIP-1α peptides were obtained from PeproTech Inc. Sch-C was synthesized using procedures analogous to those disclosed in the literature (Baroudy et al., 2000a; Palani et al., 2001). Sch-D (Tagat et al., 2004) was synthesized using procedures analogous to those disclosed in the literature (Baroudy et al., 2000b). UK-427,857 was synthesized using procedures analogous to those disclosed in the literature (Perros et al., 2001).

Results

Receptor Models Used in Analysis. The estimation of antagonist potencies and kinetics requires comparison of data with quantitative models of receptor function (see Supplemental Appendix A). In particular, the standard Ehlert (1988) model is described whereby the tracer ligand (either radioligand or functional agonist) can concomitantly bind to the receptor with the antagonist; this model predicts parallel shifts to the right of the saturation curve for a radioligand when the allosteric antagonist is present (Fig. 2A). A variant of this model is described that allows allosteric ligands to not affect the binding of agonists and radioligands but to prevent activation of the receptor by agonists. In particular, the Ehlert model predicts noncompetitive blockade of function but not binding if it is assumed that binding of the antagonist precludes receptor activation (Fig. 2B). Another model is described whereby the binding of the antagonist precludes binding of the tracer ligand in a noncompetitive manner (denoted 'noncompetitive' allosteric model) (see Supplemental Appendix B); this model predicts depression of the maxima of saturation binding curves with no concomitant dextral displacement. This model is required to describe the observed binding characteristics of these antagonists.

Two antagonist binding models (referred to as three-ligand models) also are presented to describe possible interactions between the allosteric ligands as they bind to the receptor (see *Appendix*). Finally, a new model of allosteric function presented by Hall (2000) is described as another option to account for the different characteristics of 873140 blockade of the functional effects of RANTES but not ^{125}I-RANTES binding (denoted 'Hall functional allosteric model'; see Supplemental Appendix C).

Binding of ^{125}I-MIP-1α. Saturable binding of ^{125}I-MIP-1α was obtained using an SPA. The equilibrium dissociation of ^{125}I-MIP-1α was 0.56 ± 0.08 nM (95% CI, 3.8 pM to 0.82 nM) with a maximal receptor binding of 120 fmol/mg of protein. Nonradioactive MIP-1α produced displacement of ^{125}I-MIP-1α (Fig. 3A) in an apparently competitive manner (Fig. 3B). The IC_{50} for half-maximal inhibition of binding varied with concentration of radiolabel (as expected for com-

petitive antagonism; see Fig. 3C) according to the Cheng and Prusoff (1973) correction:

$$K_B = IC_{50}/(1 + [A^*]/K_d) \quad (11)$$

where $[A^*]$ is the concentration of ^{125}I-MIP-1α, K_d is the equilibrium dissociation constant of the ^{125}I-MIP-1α /receptor complex, and IC_{50} is the molar concentration of MIP-1α producing 50% inhibition of blockade. A regression of IC_{50} values on concentration of radioligand (according to eq. 11) yielded a linear regression (Fig. 3C).

The radioligand ^{125}I-MIP-1α was displaced by TAK779 as well, but in this case, the effects seemed to be of a noncompetitive nature (Fig. 4, A and B). The IC_{50} values did not change with elevations of the concentration of radioactive label as shown in Fig. 5. This is indicative of noncompetitive antagonism whereby the magnitude of the IC_{50} value is independent of the concentration of radioligand and also is an estimate of the K_B, the equilibrium dissociation constant of the antagonist-receptor complex (for further details, see Supplemental Appendix B; Kenakin, 2004a). The mean pK_B ($-\log K_B$) for this antagonist is 7.8 ± 0.14 (95% CI, 8.1 to 7.5). A similar pattern was observed for Sch-C (SCH 351125) with noncompetitive antagonism of ^{125}I-MIP-1α binding (Fig. 4, C and D) and a pK_B of 8.2 ± 0.1 (95% CI, 8.4 to 8.0). Sch-D (SCH 417,690) also produced noncompetitive antagonism of ^{125}I-MIP-1α binding (Fig. 4, E and F) with a pK_B of 8.4 ± 0.1 (95% CI, 8.2 to 8.6). The same pattern was observed for UK-427,857 (noncompetitive antagonism of ^{125}I-MIP-1α binding; Fig. 3, G and H) with a pK_B of 8.7 ± 0.08 (95% CI, 8.5 to 8.9). For all four noncompetitive antagonists, the magnitude of the IC_{50} was not affected by the concentration of the radioligand (Fig. 5). 873140 produced noncompetitive antagonism of ^{125}I-MIP-1α binding (Fig. 6, A and B), with the IC_{50} demonstrating no effect of radioligand concentration on IC_{50} as well (see Fig. 6C). The mean value for the pK_B was 8.6 ± 0.07 (95% CI, 8.5 to 8.8). These data are summarized in Table 1.

Binding of ^{125}I-RANTES. Experiments were conducted to determine the potency of the antagonists as displacers of ^{125}I-RANTES. As seen in Fig. 7A, displacement was produced by SCh-D, TAK779, UK-427,857, and, to a very much lesser extent, 873140. It is noteworthy that the maximal displacement by each antagonist varied. A two-way analysis of variance ordering the maximal displacement produced by each antagonist as replicate sample rows versus separate antagonists as columns indicates that there was no significant variation between replicate readings for each antagonist (four separate samples measured, $F = 0.69$; df = 3,9) but a highly significant difference between antagonist type ($F = 78.2$, df = 3,9; $p < 0.0001$). These data confirm an earlier report of the same phenomenon by Maeda et al. (2004). The fact that a submaximal displacement (13%) was obtained for 873140 (compared with a nonspecific binding determined with Sch-C) is consistent with receptor system behavior according to the Ehlert model and not the noncompetitive model. Moreover, the differences in the maximal displacements indicate an allosteric mechanism and differing values of cooperativity constant α for the antagonists for RANTES interaction with CCR5.

The minimal effect of 873140 on ^{125}I-RANTES binding indicates a very weak effect of this antagonist on RANTES binding. An estimate of the quantitative difference between the allosteric effects of 873140 and the other antagonists (e.g., Sch-D), was made by projecting saturation curves for RANTES in the absence and presence of the antagonists. Figure 7B shows the specific binding of ^{125}I-RANTES and the maximal displacement of the binding of 40 pM ^{125}I-RANTES produced by 873140 and SCh-D as putative points on the allosterically shifted saturation curve in the presence of a high concentration of antagonist ($[B]/K_B \geq 300$) (see Ehlert model, Fig. 1A). It can be seen that the effects of 873140 are minimal, with an estimated α value for RANTES with this antagonist of 0.8. In contrast, the estimated minimal value for Sch-D from these data are $\alpha = 0.06$; it should be noted that, because specific binding was reduced to noise levels, the shift in the curve could be substantially greater. Therefore, 0.06 is the upper limit for the cooperativity constant for Sch-D and ^{125}I-RANTES ($\alpha \leq 0.06$). The fact that the α value for 873140 is at least 13-fold greater that Sch-D with ^{125}I-RANTES as the receptor probe indicates that different allosteric conformations are made by these antagonists (Christopoulos and Kenakin, 2002).

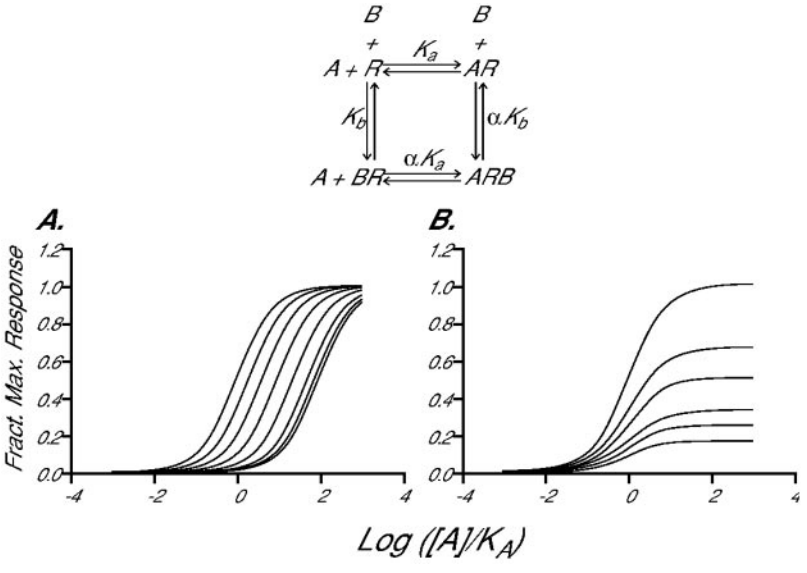

Fig. 2. Receptor species measured in a binding assay according to Ehlert (1988) in A where both the [*AR*] and the [*ABR*] species produce signals or are measured in binding experiments. Dextral displacements of the saturation binding curve (where the radioligand is [*A*]) are predicted by this model. B, noncompetitive antagonist model (only [*AR*] species is monitored) where depression of the radioligand saturation binding curve is predicted with no concomitant dextral displacement.

Kinetics of Recovery from Blockade. The effect of washing with drug-free media was explored in the ^{125}I-MIP-1α binding assay. Figure 8A shows the reversal from blockade of a single concentration of ^{125}I-MIP-1α by nonradioactive MIP-1α, SCh-C, TAK779, and 873140. As can be seen from this figure, washing over a period of 4 h at room temperature caused reversal of the binding by MIP-1α but not the allosteric antagonists. Figure 8B shows data from a differently designed experiment [i.e., with a much longer wash period (51 h)]. To preserve the viability of the receptor preparation, these studies were conducted at 4°C. The dependence of antagonist occupancy on time was assessed by subjecting the data to a *t* test for the significance of a relationship between two variables (time and occupancy) (see *Materials and Methods*). The value of *t* for the regression of ln receptor occupancy versus time showed that there was a significant effect of time on the occupancy for TAK779, Sch-C, Sch-D, MIP-1α, and UK427,857 (Table 2). In contrast, no significant relationship between the receptor occupancy of 873140 and time was observed ($p < 0.05$), indicating that this antagonist did not appreciably dissociate from the receptor over the 51-h wash period. The rates of offset for the antagonists are given in Table 2.

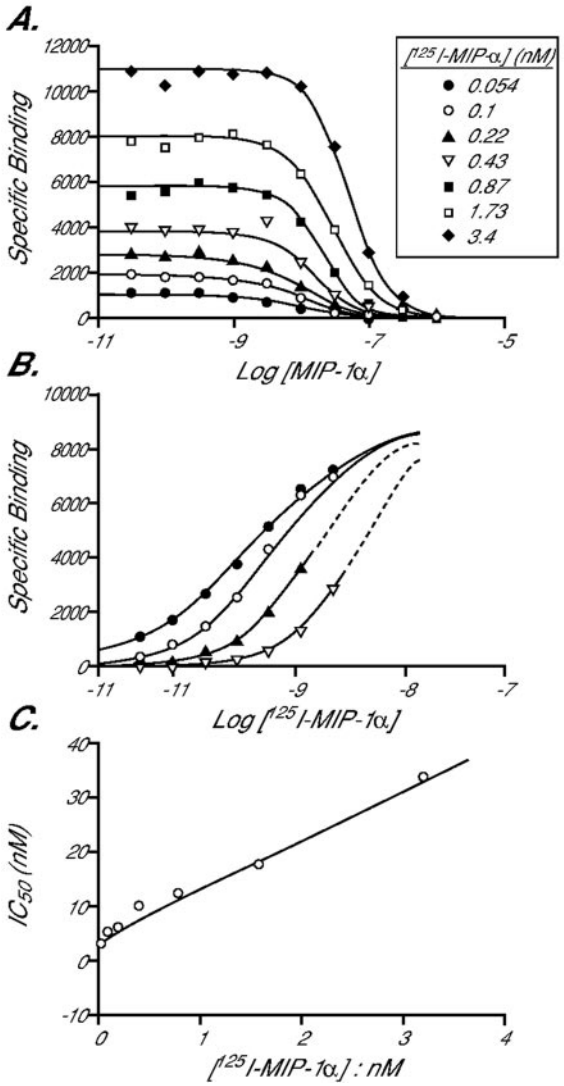

Fig. 3. Displacement of ^{125}I-MIP-1α by nonradioactive MIP-1α. A, displacement curves. Ordinates, specifically bound (to CCR5 receptor) counts per minute from ^{125}I-MIP-1α. Abscissae, molar concentrations of nonradioactive MIP-1α (logarithmic scale). Curves determined for displacement of various concentrations of ^{125}I-MIP-1α (see legend for concentrations) B, saturation binding curves for ^{125}I-MIP-1α in the absence (●) and presence of various concentrations of nonradioactive MIP-1α: 10 nM (○), 30 nM (▲), and 100 nM (△). C, relationship between observed IC_{50} for nonradioactive MIP-1α displacement of ^{125}I-MIP-1α and initial concentration of ^{125}I-MIP-1α

Functional Studies. The effect of the allosteric antagonists on calcium fluorescence responses to RANTES in HEK 293 cells transfected with CCR5 receptor were measured. As shown in Fig. 9, A–D, TAK 779, Sch-C, Sch-D, and UK427857 produced concentration-dependent noncompetitive antagonism of RANTES responses. These data were consistent with the effects of these antagonists on RANTES binding. 873140 produced blockade of calcium responses to MIP-1α (Fig. 9F), which is also consistent with the binding studies. Interestingly, however, 873140 also produced concentration-dependent noncompetitive antagonism of responses to RANTES (Fig. 9E) in stark contrast to the lack of effect of this antagonist on RANTES binding.

The depression of dose-response curves to RANTES by 873140 with no concomitant effect on binding can be predicted, under certain circumstances, by one version of the Ehlert model. In particular, if it is assumed that the allosteric modulator does not affect the binding of the agonist (or radioligand) but does prevent receptor activation by the agonist, then the effects observed for 873140 on RANTES binding and function can be accounted for. In this variant of the Ehlert model, only the [*AR*] species (receptor bound to agonist without the allosteric modulator present) produces a response. On a molecular level, this can occur if the allosteric modulator produces a conformational change in the receptor that does not interact with G-protein (Fig. 2B). The lack of effect on binding would be produced by a value for α near unity. This is consistent with the estimated value of $\alpha = 0.8$ found for 873140 and ^{125}I-RANTES binding.

This effect also can be described with a new a functional model of allosterism described by Hall (2000). This model, described in Supplemental Appendix C, indicates that receptor binding assays and receptor functional assays monitor changes in different receptor species. Therefore, a modulator that promotes radioligand binding to nonactivated receptor species while preventing the transition to activated receptor species will not affect binding but block function. An example of the use of this model to calculate the absence of significant effects on binding but a depression of function is given in Supplemental Appendix C. The important aspect of this simulation is the fact that the same antagonist (constant values of ϵ and ϕ) can produce this effect for one agonist (defined value of χ) but not another; this is consistent with the effects of 873140 with the different ligands MIP-1α and RANTES.

Allosteric Antagonist-Interactions. The possible interactions of 873140 and the other antagonists were explored by measuring the potency of 873140 (denoted as the reference antagonist) as a displacer of ^{125}I-MIP-1α in the absence and presence of a range of concentrations of each of the other antagonists (denoted the test antagonist). The presence of the test antagonist produces a diminution of the binding window for ^{125}I-MIP-1α; therefore, a concentration range of only ~10-fold can be used to determine the displacement curve of the reference antagonist. A plot of the observed IC_{50}

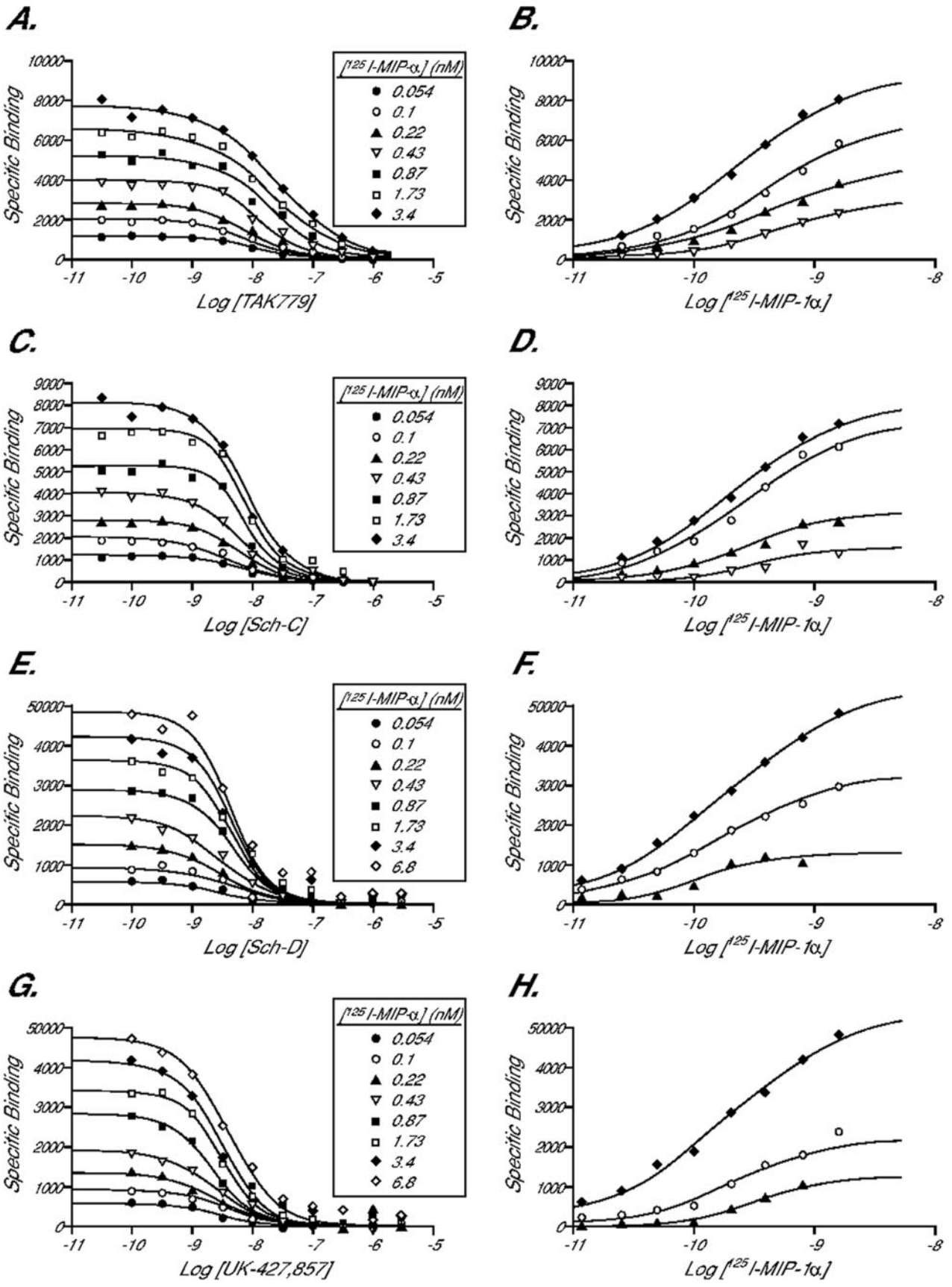

Fig. 4. Displacement of ^{125}I-MIP-1α by noncompetitive allosteric antagonists. A, TAK779 displacement curves. Ordinates, specifically bound (to CCR5 receptor) counts per minute from ^{125}I-MIP-1α. Abscissae, molar concentrations of nonradioactive TAK 779 (logarithmic scale). Curves determined for displacement of various concentration of ^{125}I-MIP-1α (see key for concentrations). B, saturation binding curves for ^{125}I-MIP-1α in the absence (●) and

values for the test antagonist in the presence of a range of concentrations of the reference antagonist versus the initial B_0 values of the ^{125}I-MIP-1α binding can be predicted from the noncompetitive allosteric model according to the following relationship (see *Appendix*):

$$\frac{B_0'}{B_0} = \frac{K_A}{IC_{50}(1-\alpha)} - \frac{\alpha}{(1-\alpha)} \quad (12)$$

where IC_{50} refers to the potency of the reference antagonist (molar concentration producing 50% displacement of the radioligand) in the presence of the test antagonist, K_A is the equilibrium dissociation constant of the reference antagonist-receptor complex (also the IC_{50} value for the reference antagonist in the absence of test antagonist for noncompetitive antagonism), and α is the cooperativity factor describing the interaction between the reference and test antagonist through the protein. The ratio B_0'/B_0 depicts the fractional decrease in basal binding produced by the test antagonist.

Various patterns for this relationship are predicted that are dependent upon whether or not the two allosteric modulators can interact (i.e., whether the binding of one allosteric modulator affects the binding of the other); these patterns are given by eq. 12; Fig. 10 shows a double logarithmic representation of this relationship under a variety of conditions. If $\alpha > 1$, the convex regression to the left reflects the fact that the binding of one allosteric modulator increases the affinity of the receptor for the other allosteric modulator. A linear vertical line indicates the condition whereby $\alpha = 1$, namely a case of completely independent binding of the two modulators. This denotes a case in which the allosteric modulators bind to their own sites on the receptor and do not affect each other, only the binding of the tracer (in this case ^{125}I-MIP-1α). A convex regression to the right denotes a case whereby the binding of one allosteric modulator negatively impacts the binding of the other ($\alpha < 1$). A linear regression with negative slope indicates a case for $\alpha = 0$, whereby the two allosteric modulators exhibit prohibitive binding. Thus, when one antagonist is bound, the affinity of the receptor for the other diminishes to very low values. The most simple case of prohibitive binding is where the antagonists bind to the same site on the receptor. It can be seen that this is predicted by the special case for eq. 12 when $\alpha = 0$ (see *Appendix*):

$$\text{Log}(B_0'/B_0) = -\text{Log}(IC_{50}/K_A) \quad (13)$$

It should be noted that, even in this scenario, the allosteric perturbation of the modulators on the receptor affecting the binding of the tracer is unique to that modulato; i.e., the effect on the tracer (either ^{125}I-MIP-1α or HIV) depends on which antagonist binds to the site. Thus, there is still allosteric texture of antagonism even if the modulators share the same allosteric binding site.

Figure 11A shows displacement curves for 873140 in the absence and presence of a range of concentrations of TAK779. It can be seen that the presence of TAK 779 reduced the binding window for the displacement curves but did not produce significant change in the IC_{50} of 873140. Figure 11B shows a regression of the log of the depression in B_0 produced by the test antagonist TAK 779 upon the log of the ratio of the IC_{50} values for 873140 in the presence and absence of TAK 779 (according to eq. 12; see *Appendix*). It can be seen that a linear relationship with a slope of −1.1 resulted (see Table 3 for quantitative data). The 95% confidence limits of the slope contain unity; therefore, these data are consistent with the model defined when $\alpha = 0$ for interaction between the two antagonists (consistent with prohibitive binding and a common binding site for the two antagonists). Figure 11, C and D, show the same data for Sch-C. It can be seen from the data in Table 3 that a common binding site ($\alpha = 0$) is indicated for 873140 and Sch-C as well. Identical qualitative results were obtained from coadministration studies with Sch-D (Fig. 11, E and F; Table 3) and UK 427,857 (Fig. 11, G and H; Table 3).

Discussion

The data described in this article are discussed in terms of an allosteric interaction between the antagonists and the chemokine radioligands. As reviewed in the introduction, the size of the proteins involved and the breadth of interaction between them would predict that steric hindrance involving the small molecule antagonists and the proteins are insufficient to account for the blockade of the protein-protein interaction. Chemokine receptors are known to function allosterically with ligands as shown in the direct kinetic binding studies between the chemokine MIP-1β and HIV envelope glycoprotein (Staudinger et al., 2001). Likewise, data from other studies implicate allosterism as a mode of action for chemokine receptors. For example, incomplete displacement of receptor radioactive peptide ligand ^{125}I-MIP-1α, a hallmark of allosteric interaction, has been observed for chemokine CCR1 receptors by the allosteric small molecule modulator UCB35625 (Sabroe et al., 2000). Likewise, different maximal displacement of chemokine ^{125}I-labeled interferon-inducible T cell α chemoattractant by the chemokine agonists 10-kDa interferon-inducible protein and monokine induced by human interferon-γ has been observed for CXCR3 receptors (Cox et al., 2001). Antibodies also have been used to discern differences in the effects of allosteric ligands. Thus, the antibody a-hCXCR3 blocks the agonist effects of the 10-kDa interferon-inducible protein but not those of interferon-inducible T cell α chemoattractant (Cox et al., 2001). Likewise, the CCR5 receptor antibody MC-1, although it blocks rather than induces chemokine response and blocks binding of chemokine to CCR5, it also actively promotes receptor internalization, a behavior usually associated with receptor activation (Blanpain et al., 2002). Finally, separate binding domains have been suggested for the small molecule antagonist Sch-C and the chemokine RANTES (Wu et al., 1997; Blanpain et al., 2003; Tsamis et al., 2003), consistent with an allosteric interaction between these ligands through the receptor.

These data are all consistent with the notion that CCR5

presence of various concentrations of TAK779: 10 nM (○), 30 nM (▲), and 100 nM (△). C, Sch-C displacement curves for concentrations of ^{125}I-MIP-1α as given in A. D, saturation binding curves for ^{125}I-MIP-1α in the absence (●) and presence of various concentrations of Sch-C (○, 3 nM; ▲, 10 nM; ▽, 30 nM). E, Sch-D displacement curves for concentrations of ^{125}I-MIP-1α as given in A. F, saturation binding curves for ^{125}I-MIP-1α in the absence (●) and presence of various concentrations of Sch-D: 3 nM (○), 10 nM (▲), and 30 nM (△). G, UK-427,857 displacement curves for concentrations of ^{125}I-MIP-1α (see key for concentrations). H, saturation binding curves for ^{125}I-MIP-1α in the absence (●) and presence of various concentrations of UK-427,857: 3 nM (○), 10 nM (▲), and 30 nM (△).

and these ligands are allosteric antagonists of CCR5. In this study, the probe dependence and saturability of the antagonism of CCR5 by 873140 strongly suggest an allosteric mode of action (Kenakin, 2004b). The most direct and compelling reason for suggesting that 873140 and the other antagonists interact with CCR5 in an allosteric fashion are the differences in binding seen with ^{125}I-MIP-1α and ^{125}I-RANTES and the concomitant striking difference between the effects on RANTES binding and function. For antagonists with an orthosteric mode of action (steric occlusion of the tracer binding site), all 'blocked' receptors can be assumed to be equal; i.e., the nature of the antagonist is immaterial because the result on the receptor is the same. In allosteric terms, 'blocked' receptors (by the antagonist) cannot be assumed to be equal because the allosteric antagonist produces a change in conformation and, as quantified by the magnitude of the cooperativity constant α, different allosteric modulators may produce different conformations of the receptor. Thus, a 'blocked' receptor simply becomes a changed receptor with its own set of affinities for various tracers (Kenakin, 2004b). In the case of 873140, the allosterically modulated receptor does not allow binding of ^{125}I-MIP-1α but does allow ^{125}I-RANTES to bind, albeit in a functionally ineffective manner. In addition, allosteric texture in the antagonism by other allosteric modulators such as Sch-C and TAK779 is demonstrated by the difference in the maximal displacement of ^{125}I-RANTES (see Fig. 9). Although inconsistent with orthosteric antagonism, this is completely consistent with an allosteric mode of action because allosteric modulation is probe-dependent; i.e., an allosteric conformational change that is catastrophic for one receptor probe may be inconsequential to another. Blockade of ^{125}I-MIP-1α binding but not ^{125}I-RANTES binding agrees with this profile of behavior.

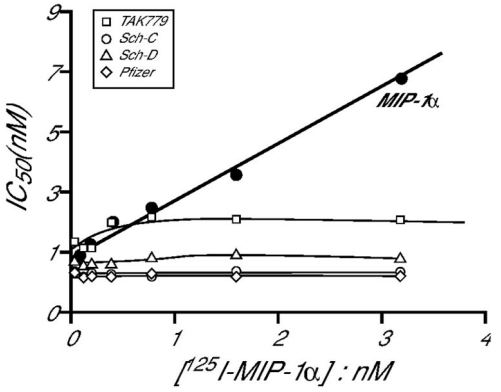

Fig. 5. Relationship between the IC_{50} for blockade of ^{125}I-MIP-1α binding (ordinates) and concentration of radioligand (abscissae). ●, MIP-1α; □, TAK779; ○, Sch-C; △, Sch-D; ◇, UK 427,857.

Although the sigmoidal displacement curves for ^{125}I-MIP-1α for the CCR5 antagonists were produced, this cannot be taken as evidence for competitive binding. In radioligand binding experiments, such curves also can result from allosteric and/or noncompetitive antagonism. An inspection of the relationship between the concentrations of radioligand bound and antagonist show a depression of the maximal binding indicative of noncompetitive antagonism. The relative geography of radioligand tracer and antagonist cannot be inferred from the displacement curves (i.e., whether the antagonist occupies the same binding site as ^{125}I-MIP-1α). The verisimilitude of the ^{125}I-RANTES binding to the pre-

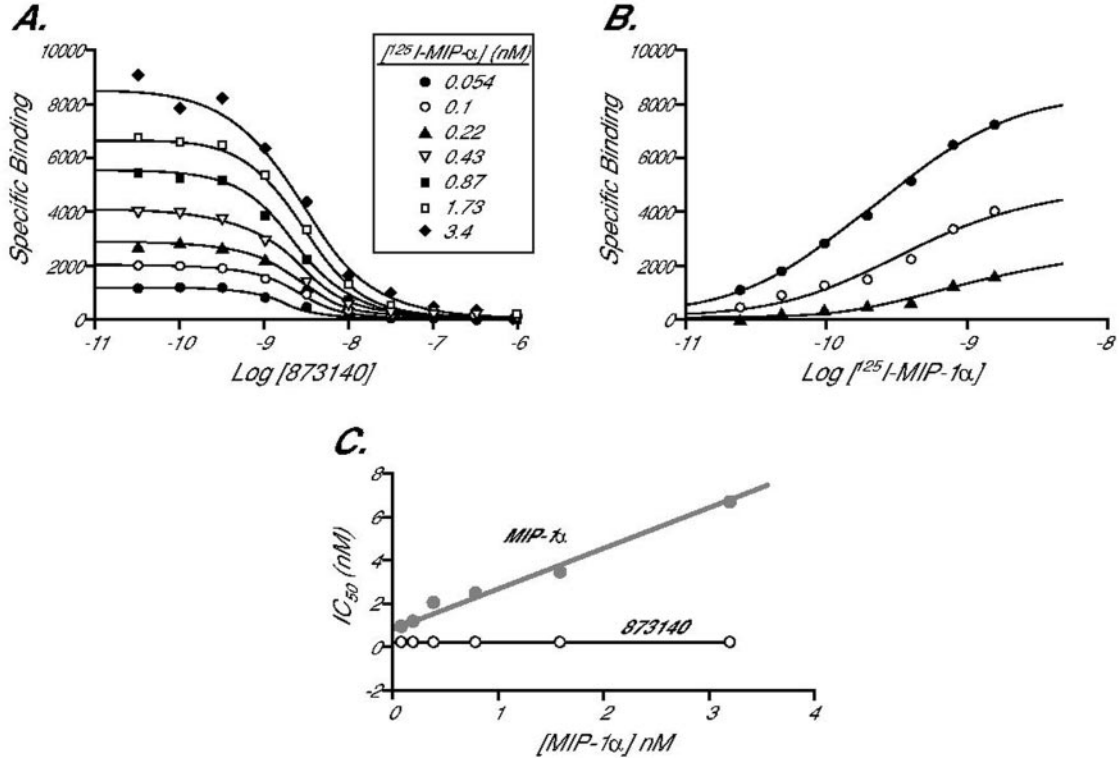

Fig. 6. Displacement of ^{125}I-MIP-1α by 873140. A, displacement curves. Ordinates, specifically bound (to CCR5 receptor) counts per minute from ^{125}I-MIP-1α. Abscissae, molar concentrations of nonradioactive 873140 (logarithmic scale). A, displacement curves for 873140 for concentrations of ^{125}I-MIP-1α as shown in key. B, saturation binding curves for ^{125}I-MIP-1α in the absence (●) and presence of various concentrations of 873140 (○, 3 nM; ▲, 10 nM). C, relationship between the IC_{50} for blockade of ^{125}I-MIP-1α binding (ordinates) and concentration of radioligand (abscissae).

diction of the Ehlert model (1988) (whereby a ternary species binds both ^{125}I-RANTES and 873140) suggests that an allosteric mechanism with separate binding sites for the antagonist and radioligand with concomitant effects transmitted through the protein is operable. In fact, Maeda and colleagues (2004) have shown the existence of such a ternary species (both radioactive RANTES and 873140 bound to the receptor simultaneously) with radiolabeled RANTES and 873140. The noncompetitive allosteric effects of 873140 as well as the other CCR5 antagonists tested in these experiments resemble the activity of the endogenous serotonin receptor tetrapeptide allosteric modulator 5-HT moduline, which reduces the maximal binding and response of serotonin for 5-HT$_{1B}$ receptors (Fillion et al., 1996; Massot et al., 1996).

A complicated pattern of behavior is demonstrated by 873140 in the lack of binding effect for ^{125}I-RANTES but blockade of RANTES function. In this case, 873140 allows RANTES to bind but not to activate G-protein to elicit re-

TABLE 1
Equilibrium dissociation constants for antagonist-CCR5 receptor complexes as measured by displacement or modification of ^{125}I-MIP-1α binding

Ligand	K_B (95% Confidence Limits)
	nM
MIP-1α	8.0 ± 1.2 (4.7–11.2)
TAK779	15.8 (7.9–31.6)
Sch-C	6.3 (4–10)
Sch-D	4.0 (2.5–6.3)
UK-427,857	2.0 (1.2–3.1)
873140	2.5 (1.6–3.2)

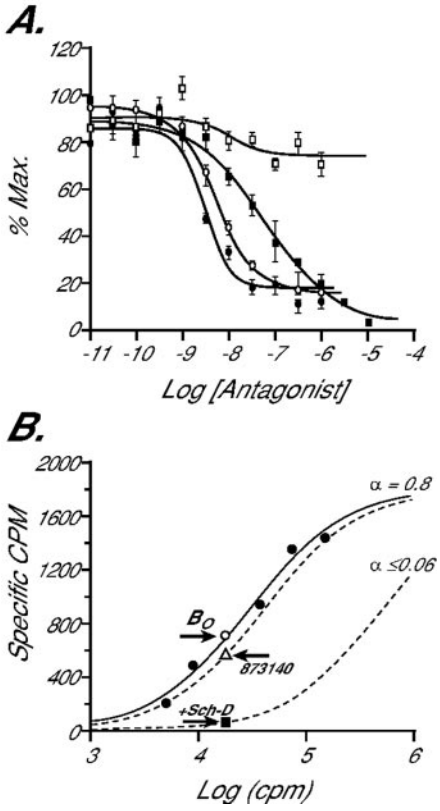

Fig. 7. Displacement of ^{125}I-RANTES from CCR5. Ordinates, counts per minute for specifically bound ^{125}I-RANTES expressed as a percentage of initial value (740 cpm). Abscissae, logarithms of molar concentrations of antagonist. A, data shown for UK-427,857 (●, n = 4), Sch-D (○, n = 4), TAK779 (■, n = 4), and 873140 (□, n = 4). Bars represent S.E.M. B, estimated dextral displacement of the saturation curve for ^{125}I-RANTES (from B_0 value for A shown as ○) produced by maximal concentrations (1 μM) of 873140 (△) and Sch-D (■). These displacements predict cooperativity constants (α) for both antagonists and RANTES (see *Appendix*). Minimal effects on RANTES binding are produced by 873140, whereas a minimal value for the displacement by Sch-D is shown (effect could be significantly greater).

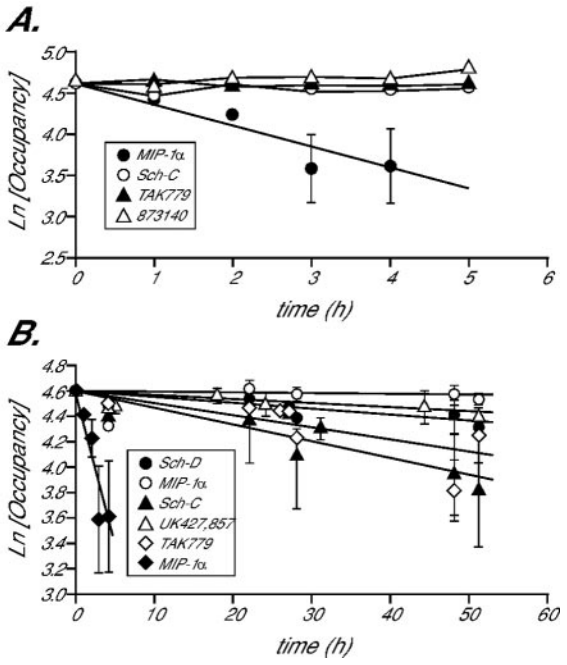

Fig. 8. Reversal of blockade by MIP-1α and allosteric antagonists with time. Ordinates, natural logarithm of the percentage of receptor occupancy by the antagonist normalized to 100% at time 0. Abscissae, time in hours. A, membranes incubated with 1 nM ^{125}I-MIP-1α in the presence of nonradioactive MIP-1α (200 nM), Sch-C (100 nM), 873140 (100 nM), and TAK779 (200 nM). Preparations were then washed for 1 to 5 h as shown, and the binding of ^{125}I-MIP-1α was measured. Key shows symbols for antagonist data. B, protocol similar to that in A, except longer wash times were used. Key shows symbols for antagonists. Data describing regressions shown in Table 2.

TABLE 2
Time course for reversal of blockade of ^{125}I-MIP-1α binding

Nonradioactive Ligand	k_{off}	95% Confidence Limits[a]	t value	Significance[b]
	h^{-1}			
MIP-1α	0.26[c]	0.22 to 0.29	8.94 df=36	$P < 0.005$
Sch-C	0.013	0.008 to 0.018	3.73 df=34	$P < 0.005$
Sch-D	0.005	0.004 to 0.006	4.45 df=34	$P < 0.005$
TAK-779	0.013	0.01 to 0.015	5.6 df=38	$P < 0.005$
UK-427,857	0.0036	0.0026 to 0.0045	3.78 df=41	$P < 0.005$
873140			0.93 df=41	N.S.

[a] 95% confidence limits of the slope from a plot of ln (receptor occupancy) vs time (hours).
[b] Value of t to determine whether a significant dependence of antagonist receptor occupancy exists on time; i.e., does washing with drug-free media cause reduction in the receptor occupancy by the antagonist? Insignificant values of t indicate no relationship between time and occupancy (i.e., operationally irreversible receptor occupancy by the antagonist over the time period of the experiment, specifically 51 h).
[c] This value was obtained at room temperature. All other values obtained at 4°C. No reversal of receptor occupancy was observed at room temperature for other antagonists at wash periods up to 8 h.

sponse. The variant of the Ehlert model whereby response is produced only by the agonist-occupied receptor (with no allosteric modulator present) predicts noncompetitive antagonism of agonist effect but no effect on the same agonist binding (as a radioligand species) if α is near unity. This effect also can be described in molecular terms with a recently described allosteric function model by Hall (2000) (see Supplemental Appendix C). In this model, receptor activation is separated from ligand binding (as in standard two-state and ternary complex models); this allows the allosteric ligand to affect activation and binding separately. In terms of this model, the key to understanding the divergence of binding and functional effects is to consider the different array of receptor species quantified by each assay. Thus, the radioligand-bound species [AR_i], [AR_a], [ABR_i], and [ABR_a] are measured for binding, whereas for function, only the activated [R_a] species are observed ([R_a], [AR_a], [BR_a], and [ABR_a]). This can lead to conditions under which no effect can be seen on radioligand bound species in the face of noncompetitive diminution of receptor function. As seen in Supplemental Appendix C, this can be modeled with an appropriate $\epsilon < 1$ with concomitant $\phi > 1$ for the antagonist; i.e., the allosteric modulator selectively binds to the inactive state of the receptor and also promotes agonist binding to the receptor. Lack of allosteric effect on binding but not function has been reported for other receptors. For example, 7-hydroxyiminocyclopropan[*b*]chromen-1a-carboxylic acid ester is a potent noncompetitive antagonist of glutamate receptor response but is also a completely ineffective displacer of glutamate binding (Litschig et al., 1999). It should be noted that the G-protein milieu surrounding the receptor is different in the binding versus functional experiments. In particular, the FLIPR experiments mediated a chimeric G-protein response opening the possibility that 873140 blocks the interaction of the receptor with the chimeric G-protein but not the natural G-protein. This possibility is made less likely by the finding of Maeda et al. (2004), which showed that 873140 blocks the chemotaxic effects of RANTES in MOLT4 cells. It should also be noted that if the Hall model were operative (i.e., $\epsilon < 1$), 873140 would demonstrate inverse agonist properties in constitutively active receptor systems. Whether 873140 is an inverse agonist remains unknown.

The coadministration studies are consistent with the idea that 873140 and the other antagonists bind to a common allosteric binding site on the receptor (i.e., α for the coadministration model $\rightarrow 0$). This should not be interpreted to suggest that these antagonists have the same effect on the receptor to achieve prevention of HIV entry. This latter

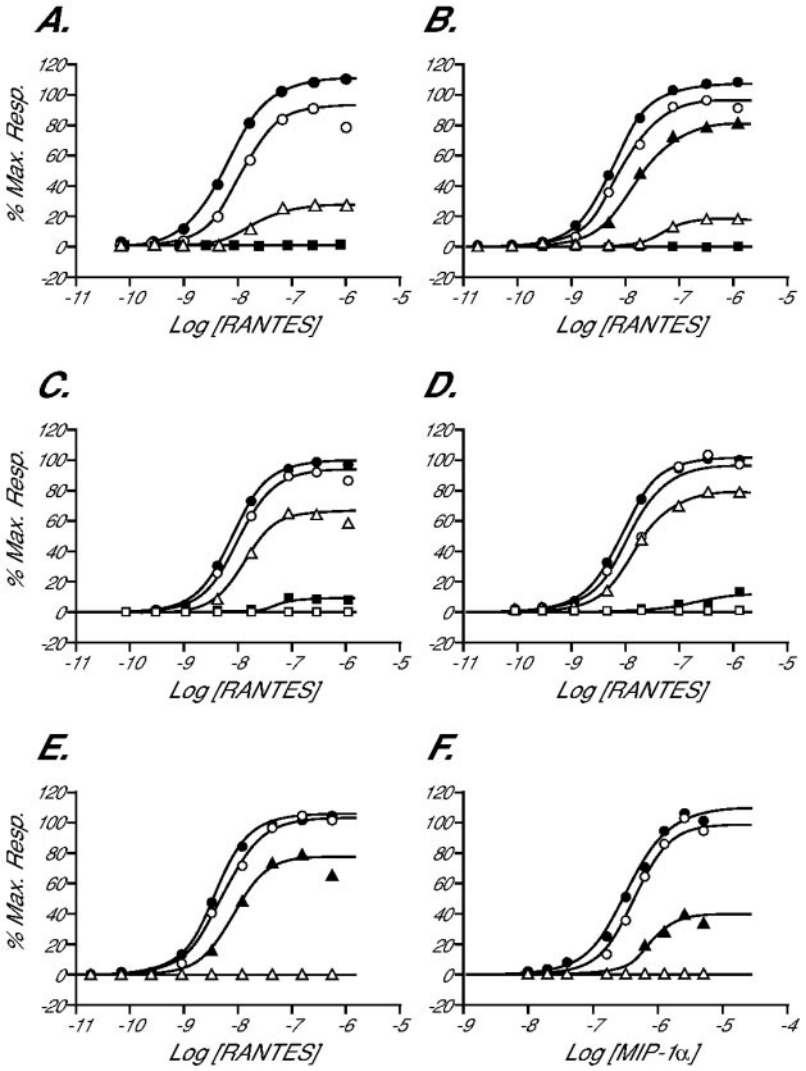

Fig. 9. Calcium responses to chemokine agonists RANTES (A–E) and MIP-1α (F). Ordinates, percentage of maximal response to the agonist. Abscissae, logarithms of molar concentration of agonist. A, responses in the absence (●, $n = 4$) and presence of TAK 779: 3 nM (○), 10 nM (△), and 30 nM (■) ($n = 4$). A, responses in the absence (●) and presence of Sch-C: 10 nM (○), 30 nM (▲), and 100 nM (△) ($n = 3$). C, responses in the absence (●) and presence of Sch-D: 3 nM (○), 10 nM (△), and 30 nM (■) ($n = 5$). D, responses in the absence (●, $n = 4$) and presence of UK-427,857: 0.3 nM (○), 1 nM (△), 3 nM (■), and 10 nM (□) ($n = 4$). E, responses in the absence (●) and presence of 873140: 1 nM (○), 3 nM (▲), and 10 nM (△) ($n = 3$). F, responses to MIP-1α in the absence (●) and presence of 873140: 1 nM (○), 3 nM (▲), and 10 nM (△) ($n = 5$).

property is controlled by the co-operativity factors for HIV, not other antagonists (i.e., each antagonist prevents HIV fusion by inducing its own effect on the receptor. This idea is underscored by the differences in the binding of with ^{125}I-MIP-1α and ^{125}I-RANTES produced by the various antagonists; i.e., whereas Sch-C blocks both ^{125}I-MIP-1α and ^{125}I-RANTES, 873140 blocks only the binding of ^{125}I-MIP-1α.

There are therapeutic implications of an allosteric mechanism that pertain to the use of these antagonists in the treatment of HIV. Long-term treatment with a CCR5 antagonist might select for gp120 variants able to infect cells via binding to allosterically modified receptor. HIV-1 is known to mutate, resulting in sequence changes in its Env complex with no concomitant loss of function (Wyatt and Sodroski, 1998; Poignard et al., 2001). Passage studies with AD101, an antagonist structurally related to Sch-C, have indicated that resistance can occur through the production of an escape mutant in the presence of antagonist (Trkola et al., 2002; Kuhmann et al., 2004). If another allosteric antagonist induces a different conformation, then it is possible that the mutant virus would not be cross-resistant to both drugs. It is interesting to note that mutation studies on the Sch-C analog AD101-resistant escape mutant virus CC101.19 indicate that the four amino acid substitutions on the V3 loop of gp120 require the native three-dimensional presentation to the receptor to confer resistance (Kuhmann et al., 2004); this would suggest that allosteric conformational changes may be effective in disrupting the tertiary interaction of the gp-120 and CCR5 interfaces. This would offer a treatment option after the emergence of resistance to the first agent. With regard to 873140, this idea is supported directly by a recent report by Maeda et al. (2004) who show that 873140 produces a different profile for antibody binding to CCR5 than does Sch-C or TAK-779. Likewise, although the COC101.19 escape mutant virus is insensitive to the small molecule AD101, it is sensitive to the chemokine RANTES (Kuhmann et al., 2004). These data suggest that the conformation produced by AD101 differs from that made by RANTES (an agonist that promotes coupling of G-proteins to CCR5). This is consistent with the notion that different CCR5 conformations will present problematic receptor conformations to resistant viruses.

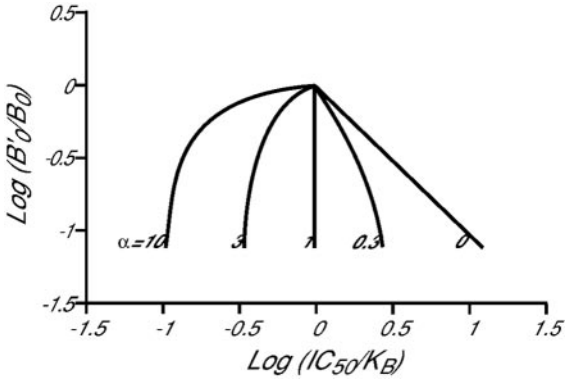

Fig. 10. Coadministration of two allosteric modulators (a test antagonist and a reference antagonist). Ordinates, relative initial level of binding of the tracer in the presence of the test antagonist (as a fraction of the initial level of binding in the absence of any antagonist). Abscissae, the ratio of the IC_{50} values of the reference antagonist (for displacement binding) in the presence of various concentrations of test antagonist. The scales for both the ordinate and the abscissa are logarithmic. Model described fully in *Appendix*.

The offset experiments showed a difference between the rate of offset of the noncompetitive antagonists and the peptide chemokine MIP-1α. No offset of the noncompetitive antagonists was observed at room temperature for 5 h, precluding direct comparison with MIP-1α. However, an internal comparison of the noncompetitive antagonists was done under identical conditions; the comparison of the mean rates and 95% confidence limits of the estimates indicated three general groups. The antagonists with the most rapid offset were Sch-C and TAK779. A statistically slower set of offset rates was obtained for Sch-D and UK427,857. Finally, no significant offset over the 51- h time period was observed for 873140. It is not possible to determine a half-time for reversal of receptor antagonism for 873140 from these data because the statistical significance of time dependence depends both upon the slope of the offset line and the scatter in the data. To calculate a half-time under these conditions, a measurable offset for 873140 would need to be determined under these experimental circumstances. However, we can estimate the lower limit of the half-time from the measured offset of UK 427,857. The data in Fig. 8 indicate that the half-time for reversal of UK 427,857 antagonism of CCR5 is 136 h. Because the offset of 873140 is measurably slower than that obtained for UK 427,857 under these experimental conditions, it can be estimated that the half-time for reversal of 873140 is >136 h. It would be predicted that protection from HIV infection requires constant allosteric modulation of the receptor; therefore, the particularly persistent antagonism of CCR5 by 873140 suggests that this ligand may have a therapeutic advantage over more labile (higher rate of offset from the receptor) antagonists. In view of the inordinately slow offset from the receptor ($<0.004\ h^{-1}$) after exposure to 873140, infectability may depend more on the generation of new CCR5 receptors on the cell surface than on offset of 873140.

In general, 873140 demonstrates characteristics of CCR5 receptor blockade similar to those of other CCR5 antagonists found to reduce HIV viral load in humans. In addition, the fact that this is an allosteric ligand that produces a receptor conformation different from that produced by other antagonists suggests that this ligand may yield a unique viral resistance profile. It will be interesting to determine whether the unusually slow offset of 873140 from the receptor will translate into a unique therapeutic profile for this molecule.

Appendix

Three Ligand Interactions

Allosteric Noncompetitive Interactive. Receptor interacts with virus ([*V*]), and two noncompetitive ligands [*A*] and [*B*]. Each antagonist binds to its own binding site and the binding of one allosteric antagonist affects the binding of the other by a cooperativity factor α (Scheme 1).

$$[AR] = [ABR]/(\alpha[B]K_b) \quad (14)$$

$$[BR] = [ABR]/(\alpha[A]K_a) \quad (15)$$

$$[R] = [ABR]/(\alpha[A]K_a[B]K_b) \quad (16)$$

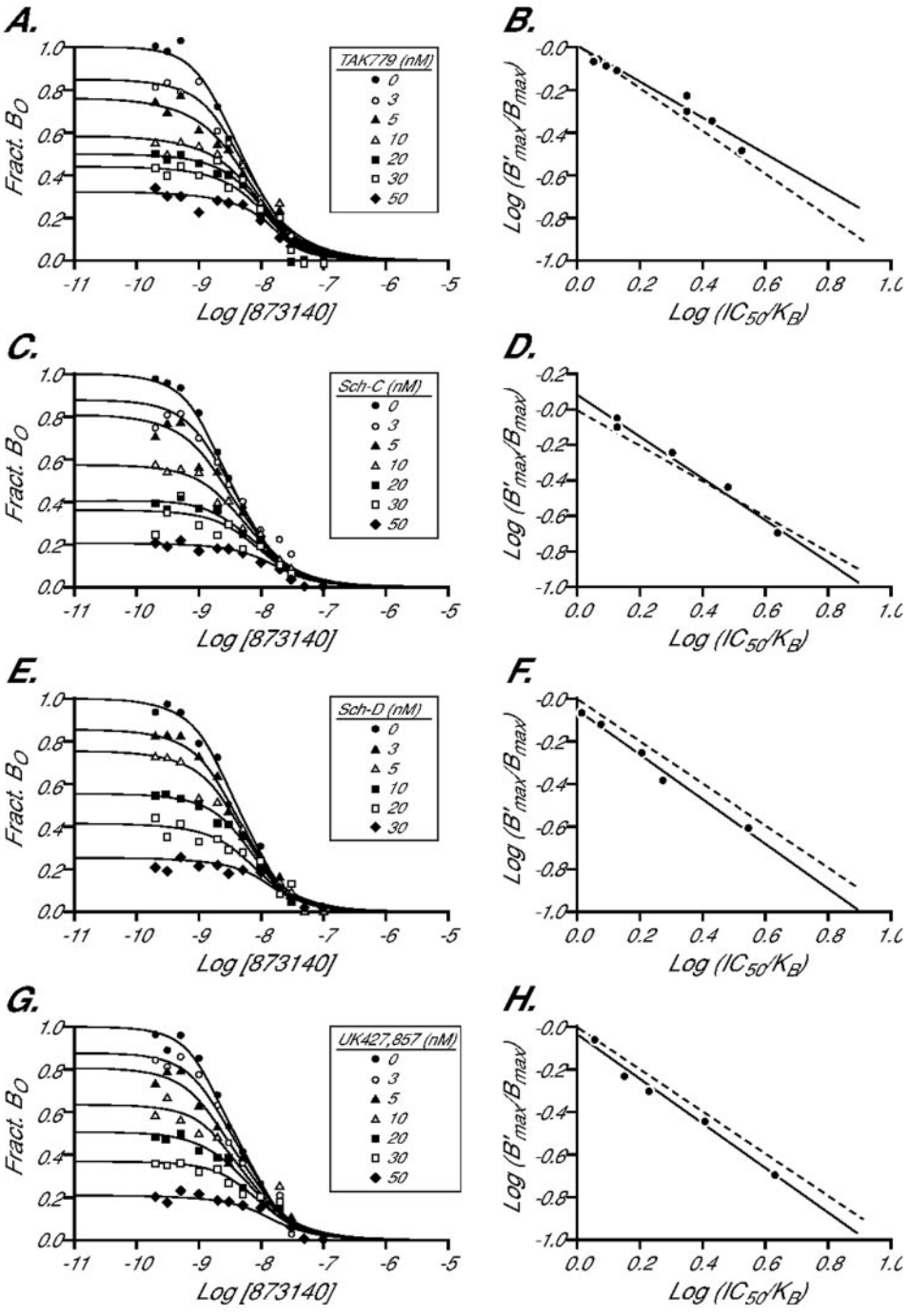

Fig. 11. Displacement of bound ^{125}I-MIP-1α by 873140 in the absence (●) and presence of a test antagonist. Keys show concentrations of antagonists. A, test antagonist is TAK779. B, regression of basal binding levels of ^{125}I-MIP-1α (ordinates) and observed potency (log IC_{50} values) of 873140 according to eq. 12. Solid line represents best linear least-squares fit of data points; dotted line represents a line of slope equal to −1. Data characterizing regression shown in Table 3. C, test antagonist is Sch-C. D, regression according to eq. 12 as for B for Sch-C; data describing regression shown in Table 3. E, test antagonist is Sch-D. F, regression according to eq. 12 as for B for Sch-D; data describing regression in Table 3. G, test antagonist is UK-427,857. H, regression according to eq. 12 as for B for UK-427,857; data describing regression in Table 3.

TABLE 3
Relationship between potency of 873140 in the presence of test antagonists

Test Antagonist	*t* Value[a]	Significance	Slope[b]	95% Confidence Limits of Slope
TAK 779	8.17	$P < 0.0005$	−0.84	−1.1 to −0.55
Sch-C	14.2	$P < 0.0005$	−1.18	−1.1 to −0.9
Sch-D	15.1	$P < 0.0005$	−1.1	−1.3 to −0.84
UK-427,857	14.8	$P < 0.0005$	−1.0	−1.3 to −0.8

[a] Measure of the significance of a possible relationship between *x* and *y* values. In this case, *x* is the log of the ratio of IC_{50} values for the reference antagonist in the presence and absence of test antagonist (abscissae as for Fig. 11) and *y* is the log of the ratio of B_0 values in the presence and absence of test antagonist (ordinates as for Fig. 11). See *Materials and Methods* for further details.
[b] Slope of the regression of *x* and *y* as shown in Fig. 11.

The occupancy by antagonists A and B as a fraction of total receptor occupancy (converting association equilibrium constants K_a and K_b to dissociation constants) is given by:

$$\rho_{AB} = \frac{[A]/K_A(1 + \alpha[B]/K_B) + [B]/K_B}{[A]/K_A(1 + \alpha[B]/K_B) + [B]/K_B + 1} \quad (17)$$

The fractional occupancy by tracer (such as ^{125}I-MIP-1α) is given by:

$$\rho_t = \frac{[\text{tracer}]/K_t}{([\text{tracer}]/K_t) + 1}(1 - \rho_{\text{Antagonist}}) \quad (18)$$

where $\rho_{\text{Antagonist}}$ is the fractional receptor occupancy by the noncompetitive antagonist. Mass action for receptor occupancy by antagonist [*A*] predicts:

$$(1 - \rho_A) = (1 + [A]/K_A)^{-1} \quad (19)$$

Likewise, from eq. 17:

$$(1 - \rho_{AB}) = ([A]/K_A(1 + \alpha[B]/K_B) + [B]/K_B + 1)^{-1} \quad (20)$$

The occupancy of the receptor by a tracer molecule at any concentration [tracer] is given by eq. 17. Comparing receptor occupancy for a tracer in the presence of antagonist [*A*] as a fraction of the occupancy of the tracer in the absence of [*A*] and letting [*A*] equal the IC_{50} of the test antagonist [*A*] yields:

$$0.5 = \frac{1 + [IC_{50}]/K_A}{[IC_{50}]/K_A(1 + \alpha[B]/K_B) + [B]/K_B + 1} \quad (21)$$

which leads to:

$$\frac{IC_{50}}{K_A} = \text{Ratio}_I = \frac{(1 + [B]/K_B)}{(1 + \alpha[B]/K_B)} \quad (22)$$

It can be seen that if the sites are mutually exclusive (either binding of *A* precludes the binding of *B* and vice versa, such as would be obtained with a single binding site for both), then $\alpha = 0$. This can be shown independently as shown below.

Allosteric Noncompetitive Noninteractive. Receptor interacts with virus ([*V*]), and two noncompetitive ligands [*A*] and [*B*] such that the binding of *A* precludes binding of *B* and vice versa (Scheme 2).

$$[R] = [AR]/[A]K_a \quad (23)$$

$$[BR] = [B]K_b[AR]/[A]K_a \quad (24)$$

Fractional receptor occupancy by [A] and [B] is given by:

$$\rho = [AR] + [BR]/([AR] + [BR] + [R]) \quad (25)$$

Converting association equilibrium constants K_a and K_b to dissociation constants this is given by:

$$\rho_{AB} = \frac{[A]/K_A + [B]/K_B}{[A]/K_A + [B]/K_B + 1} \quad (26)$$

The fractional occupancy by virus is given by:

$$\rho_V = \frac{[V]/K_V}{[V]/K_V + 1}(1 - \rho_{\text{Antagonist}}) \quad (27)$$

where $\rho_{\text{Antagonist}}$ is the fractional receptor occupancy by the noncompetitive antagonist. The IC_{50} for antagonist [A] is given by the ratio of tracer occupancy in the presence of both A+B and B.

$$IC_{50} = \rho_t(1 - \rho_{AB})/\rho_t(1 - \rho_B) = K_A(1 + [B]/K_B) \quad (28)$$

It can be seen that eq. 28 is eq. 22 when $\alpha = 0$ in accordance with the fact that $\alpha = 0$ represents the special case where there is no interaction between ligands A and B in the interactive model.

Relationship between B_0 and IC_{50} with Antagonist Coadministration. Eq. 22 can be used to determine the relationship between the effect of the test antagonist on resting level of radioligand binding and observed potency of the reference antagonist obtained in the presence of various concentrations of test antagonist.

The bound basal tracer binding in the absence of the test antagonist is defined as B_0 and is given by mass action.

$$B_0 = \frac{[\text{tracer}]}{[\text{tracer}] + K_d} \quad (29)$$

where K_d is the equilibrium dissociation constant of the tracer molecule-receptor complex. The binding in the presence of a pre-equilibrated concentration of test noncompetitive antagonist is defined as B_0' and is given as:

$$B_0' = \frac{[\text{tracer}]}{[\text{tracer}] + K_d}(1 - \rho_{\text{Antagonist}}) \quad (30)$$

where $\rho_{\text{Antagonist}}$ is the fractional receptor occupancy by the antagonist given by:

$$\rho_{\text{Antagonist}} = \frac{[B]/K_B}{[B]/K_B + 1} \quad (31)$$

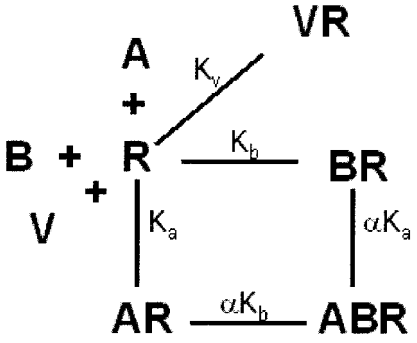

Scheme 1.

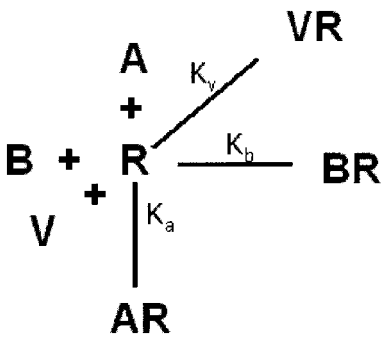

Scheme 2.

The ratio of tracer binding levels in the presence and absence of the noncompetitive antagonist is given by B_0'/B_0 and, substituting from eq. 31, it can be shown that:

$$\frac{[B]}{K_B} = \frac{(1 - (B_0'/B_0))}{B_0'/B_0} \quad (32)$$

Substituting for $[B]/K_B$ in eq. 22 yields:

$$\frac{B_0'}{B_0} = \frac{K_A}{IC_{50}(1-\alpha)} - \frac{\alpha}{(1-\alpha)} \quad (33)$$

It can be seen from eq. 33 that when $\alpha = 0$ (both antagonists bind to a common site or the binding of one antagonist precludes binding of the other at the same time), the logarithmic metameter yields a straight line with a slope of negative one.

$$\text{Log}(B_0'/B_0) = -\text{Log}(IC_{50}/K_A) \quad (34)$$

Acknowledgments

We thank Cecilia Koble, Neil Bifulco, and Virgil Styles for synthesizing Sch-C, Sch-D, and UK 427,857. We also thank Larry Boone (Dept of Virology) for very useful input into the manuscript. We also especially thank Shiro Shibayama and Kenji Sagawa of ONO Pharmaceutical Company for valuable comments on these experiments and this article.

References

Alkhatib G, Combadiere C, Broder CC, Feng Y, Kennedy PE, Murphy PM, and Berger EA (1996) CC CKR5: A RANTES, MIP-1, MIP-1 receptor as a fusion cofactor for macrophage-tropic HIV-1. *Science (Wash DC)* **272:**1955–1958.

Atchison RE, Gosling J, Monteclaro FS, Franci C, Digilio L, Charo IF, and Goldsmith M (1996) Multiple extracellular elements of CCR5 and HIV-1 entry: dissociation from response to chemokines. *Science (Wash DC)* **274:**1924–1926.

Baba M, Nishimura O, Kanzaki N, Okamoto M, Sawad H, Iizawa Y, Shiraishi M, Aramaki Y, Okonogi K, Ogawa Y, et al. (1999) A small-molecule, nonpeptide CCR5 antagonist with highly potent and selective anti-HIV-1 activity. *Proc Natl Acad Sci USA* **96:**5698–5703.

Baroudy B, Clader JW, Josien HB, McCombie SW, McKittrick BA, Miller MW, Neustadt BR, Palani A, Steensma R, Tagat JR, et al. (2000a) PCT Int. Appl. WO 2000066559.

Baroudy BM, Clader JW, Josien HB, Mccombie SW, Mckittrick BA, Miller MW, Neustadt BR, Palani A, Smith EM, Steensma R, et al. (2000b) PCT Int. Appl., WO 2000066558.

Bieniasz PD, Fridell RA, Aramori I, Ferguson SS, Caron MG, and Cullen BR (1997) Multiple active states and oligomerization of CCR5 revealed by functional properties of monoclonal antibodies. *EMBO (Eur Mol Biol Organ) J* **16:**2599–2609.

Blanpain C, Vanderwinden J-M, Cihak J, Wittamer V, Le Poul E, Issafras H, Strangassinger M, Vassart G, Marullo S, Schlondorff D, et al. (2002) Multiple active states and oligomerization of CCR5 revealed by functional properties of monoclonal antibodies. *Mol Biol Cell* **13:**723–737.

Blanpain C, Doranz BJ, Bondue A, Govaerts C, De Leener A, Vassart G, Doms RW, Proudfoot A, and Parmetier M (2003) The core domain of chemokines binds CCR5 extracellular domains while their amino terminus interacts with the transmembrane helix bundle. *J Biol Chem* **278:**5179–5187.

Cheng YC and Prusoff WH (1973) Relationship between the inhibition constant (Ki) and the concentration of inhibitor which causes 50 percent inhibition (I50) of an enzymatic reaction. *Biochem Pharmacol* **22:**3099–3108.

Choe H, Farzan M, Sun Y, Sullivan N, Rollins B, Ponath PD, Wu L, MacKay CR, LaRosa G, Newman G, et al. (1996) The β-chemokine receptors CCR3 and CCR5 facilitate infection by primary HIV-1 isolates. *Cell* **85:**1135–1148.

Christopolous A and Kenakin TP (2002) G-protein coupled receptor allosterism and complexing. *Pharmacol Rev* **54:**323–374.

Conklin BR, Farfel Z, Lustig KD, Julius D, and Bourne HR (1993) Substitution of three amino acids switches receptor specificity of Gq alpha to that of Gi alpha. *Nature* (*Lond*) **363:**274–276.

Cox MA, Jenh C-H, Gonsiorek W, Fine J, Narula SK, Zavodny PJ, and Hipkin RW (2001) Human interferon-inducible 10-kDa protein and human interferon-inducible T cell α chemoattractant are allotopic ligands for human CXCR3: differential binding to receptor states. *Mol Pharmacol* **59:**707–715.

Demarest J, Adkison K, Sparks S, Shachoy-Clark A, Schell K, Reddy S, Fang L, O'Mara K, Shibayama S, and Piscitelli S (2004) Single and multiple dose escalation study to investigate the safety, pharmacokinetics and receptor binding of 873140, a novel CCR5 receptor antagonist, in healthy subjects. Abstract 139. 11th Conference on Retroviruses and Opportunistic Infections; 2004 Feb 8–11; San Francisco, California.

Demarest J, Shibayama S, Ferris R, Vavro C, St. Clair M, and Boone L (2004) A novel CCR5 antagonist, 873140, exhibits potent in vitro anti-HIV activity. Abstract WeOrA1231. The XV International AIDS Conference; 2004 Jul 11–16; Bangkok, Thailand.

Deng H, Unutmaz D, Kewalramani VN, and Littman DR (1997) Expression cloning of new receptors used by simian and human immunodeficiency viruses. *Nature (Lond)* **388:**296–300.

Doms RW and Peiper SC (1997) Unwelcomed guests with master keys: how HIV uses chemokine receptors for cellular entry. *Virol* **235:**179–190.

Doranz BJ, Lu Z-H, Rucker J, Zhang T-Y, Sharron M, Cen Y-H, Wang Z-X, Guo H-H, Du J-D, Accavitti MA, et al. (1997) Two distinct CCR5 domains can mediate coreceptor usage by human immunodeficiency virus type 1 *J Virol* **71:**6305–6314.

Doranz BJ, Rucker J, Smyth Y, Samson RJ, Peiper SC, Parmentier M, Collman RG, and Doms RW (1996) A dual-tropic primary HIV-1 isolate that uses fusin and the β-chemokine receptors CKR-5, CKR-3 and CKR-2b as fusion cofactors. *Cell* **85:**1149–1158.

Dragic T, Trkola A, Thompson DA, Cormier EG, Kajumo FA, Maxwell E, Lin SW, Ying W, Smith SO, Sakmar SP, et al. (2000) A binding pocket for a small molecule inhibitor of HIV-1 entry within the transmembrane helices of CCR5. *Proc Natl Acad Sci USA* **97:**5639–5644.

Ehlert FJ (1988) Estimation of the affinities of allosteric ligands using radioligand binding and pharmacological null methods. *Mol Pharmacol* **33:**187–194.

Fillion G, Rousselle JC, Massot O, Zifa E, Fillion MP, and Prudhomme N (1996) A new peptide, 5-HT moduline, isolated and purified mammalian brain specifically interacts with 5-HT1B/1D receptors. *Behav Brain Res* **73:**313–317.

Finke PE, Oates B, Mills SG, MacCross M, Malkowitz L, Springer MS, Gould SL, DeMartino JA, Carella A, Carver G, et al. (2001) Antagonists of the human CCR5 receptor as anti-HIV-1 agents. Part 4: synthesis and structure-activity relationships for 1-[*N*-(methyl)-*N*-(phenylsulfonyl)amino]-2-(phenyl)-4-(4-(*N*-(alkyl)-*N*-(benzyloxycarbonyl)amino)piperidin-1-yl)butanes. *Bioorg Med Chem Lett* **11:**2475–2479.

Hall DA (2000) Modeling the functional effects of allosteric modulators at pharmacological receptors: an extension of the two-state model of receptor activation. *Mol Pharmacol* **58:**1412–1423.

Kazmierski WM, Bifulco N, Yang H, Boone L, DeAnda F, Watson C, and Kenakin T (2003) Recent progress in discovery of small-molecule CCR5 Chemokine receptor ligands as HIV-1 inhibitors. *Bioorg Med Chem* **11:**2663–2676.

Kazmierski WM, Boone L, Lawrence W, Watson C, and Kenakin T. CCR5 chemokine receptors: gatekeepers of HIV-1 infection (2002) *Curr Drug Targets Infect Disord* **2:**265–278.

Kenakin TP (2004a) *A Pharmacology Primer: Theory, Application and Methods*. Academic Press, San Diego, CA.

Kenakin TP (2004b) Allosteric modulators; the new generation of receptor antagonist. *Mol Interv* **4:**222–229.

Kuhmann SE, Pugach P, Kunstman KJ, Taylor J, Stanfield RL, Snyder A, Strizki JM, Riley J, Baroudy BM, Wilson IA, et al. (2004) Genetic and phenotypic analyses of human immunodeficiency virus type 1 escape form small-molecule CCR inhibitor. *J Virol* **78:**2790–2807.

Kwong PD, Wyatt R, Robinson J, Sweet RW, Sodroski J, and Hendricks WA (1998) Structure of an HIV gp120 envelope glycoprotein in complex with the CD4 receptor and a neutralizing human antibody *Nature (Lond)* **393:**648–659.

Lee B, Sharron M, Blanpain C, Doranz BJ, Vakili J, Setoh P, Berg E, Liu G, Guy HR, Durell R, et al. (1999) Epitope mapping of CCR5 reveals multiple conformational states and distinct but overlapping structures involved in chemokine and coreceptor function. *J Biol Chem* **274:**9617–9626.

Litschig S, Gasparini F, Rueegg DF, Stoehr N, Flor PJ, Vranesic I, Prézeau L, Pin JP, Thomsen C, and Kuhn R (1999) CPCCOEt, a noncompetitive metabotropic glutamate 1 receptor antagonist, inhibits receptor signaling without affecting glutamate binding. *Mol Pharmacol* **55:**453–461.

Luckow VA, Lee SC, Barry GF, and Olis PO (1993) Efficient generation of infectious recombinant baculoviruses by site-specific transposon-mediated insertion of foreign genes into a baculovirus genome propagated in *Escherichia coli*. *J Virol* **67:**4566–4579.

Maeda K, Nakata H, Koh Y, Miyakawa T, Ogata H, Takaoka Y, Sbibayama S, Sagawa K, Fukushima D, Moravek J, et al. (2004) Spirodiketopiperazine-based CCR5 inhibitor which preserves CC-chemokine/CCR5 interactions and exerts potent activity against R5 human immunodeficiency virus type 1 *in vitro*. *J Virol* **78:**8654–8662.

Massot O, Rouselle JC, Fillion MP, Grimaldi B, Cloez-Tayarani I, Fugelli A, Prudhomme N, Segun L, Rousseau B, Plantefol M, et al. (1996) 5-Hydroxytryptamine-moduline, a new endogenous cerebral peptide, controls the serotonergic activity via its specific interaction with 5-hydroxytryptamine $_{1B/1D}$ receptors. *Mol Pharmacol* **50:**752–762.

O'Reilly DR, Miller LK, and Luckow VA (1992) *Baculovirus Expression Vectors: a Laboratory Manual*. Oxford University Press, New York.

Palani A, Shapiro S, Clader JW, Greenlee WJ, Cox K, Strizki J, Endres M, and Baroudy BH (2001) Discovery of 4-[(*Z*)-(4-bromophenyl)-(ethoxyimino)methyl]-1′-[(2,4-dimethyl-3-pyridinyl)carbonyl]-4′-methyl-1,4′- bipiperidine-*N*-oxide (SCH 351125): an orally bioavailable human CCR5 antagonist for the treatment of HIV infection. *J Med Chem* **44:**3339–3342.

Perros M, Price DA, Stammen BL, Wood A. PCT Int. Appl. (2001), WO 2001090106.

Picard L, Simmons G, Power CA, Meyer A, Wiess RA, and Clapham PR (1997) Multiple extracellular domains of CCR-5 contribute to human immunodeficiency virus type 1 entry and fusion *J Virol* **71:**5003–5011.

Poignard P, Saphire EO, Parren PW, and Burton DR (2001) gp120: biologic aspects of structural features. *Annu Rev Immunol* **19:**253–274.

Rizzuto CD, Wyatt R, Hernández-Ramos N, Sun Y, Kwong PD. Hendrickson WA and Sodroski J (1998) A conserved HIV gp120 glycoprotein structure involved in chemokine receptor binding. *Science (Wash DC)* **280:**1949–1953.

Ross T, Bieniasz PD, and Cullen BR (1999) Role of chemokine receptors in HIV-1 infection and pathogenesis *Adv Virus Res* **52:**233–267.

Rucker J, Edinger AL, Sharron M, Samson M, Lee B, Berson JFY, Collman RG, Doranz BJ, Doms RW, and Parmentier M (1997) Utilization of chemokine recep-

tors, orphan receptors and herpesvirus- encoded receptors by diverse human and simian immunodeficiency viruses *J Virol* **71:**8999–9007.
Sabroe I, Peck MJ, Van Keulen BJ, Jorritsma A, Simmons G, Clapham PR, Williams TJ, and Pease JE (2000) A small molecule antagonist of chemokine receptors CCR1 and CCR3. *J Biol Chem* **275:**25985–25992.
Shieh JTC, Albright AV, Sharron M, Gartner S, Stritzki J, Doms RW, and Gonzalez-Scarano F (1998) Chemokine receptor utilization by human immunodeficiency virus type 1 isolates that replicate in microglia. *J Virol* **72:**4243–4249.
Smyth RJ, Yi Y, Singh A, and Collman RG (1998) Determinants of entry cofactor utilization and tropism in a dualtropic human immunodeficiency virus type 1 primary isolate. *J Virol* **72:**4478–4484.
Staudinger R, Wang X, and Bandres JC (2001) Allosteric regulation of CCR5 by guanine nucleotides and HIV-1 envelope. *Biochem Biophys Res Commun* **286:**41–47.
Strizki JM, Xu S, Wagner NE, Wojcik L, Liu J, Hou Y, Endres M, Anandan P, Shapiro S, Clader JW, et al. (2001) SCH-C (SCH 351125), an orally bioavailable, small molecule antagonist of the chemokine receptor CCR5, is a potent inhibitor of HIV-1 infection in vitro and in vivo. *Proc Natl Acad Sci USA* **98:**12718–12723.
Tagat JR, McCombie SW, Nazareno D, Labroli MA, Xiao Y, Steensma RW, Strizki JM, Baroudy BM, Cox K, Lachowicz J, et al. (2004) Piperazine-based CCR5 antagonists as HIV-1 inhibitors. IV. Discovery of 1-[(4,6-dimethyl-5-pyrimidinyl)carbonyl]-4-[4-{2-methoxy-1(R)-4-(trifluoromethyl) phenyl}ethyl-3(S)-methyl-1-piperazinyl]-4-methylpiperidine (Sch-417690/Sch-D), a potent, highly selective and orally bioavailable CCR5 antagonist. *J Med Chem* **47:**2405–2408.
Trkola A, Kuhmann SE, Strizki JM, Maxwell E, Ketas T, Morgan T, Pugach P, Xu S, Wojcik L, Tagat J, et al. (2002) HIV-1 escape from a small molecule, CCR5-specific entry inhibitor does not involve CXCR4 use. *Proc Natl Acad Sci USA* **99:**395–400.
Tsamis F, Gavrilov S, Kajumo F, Seibert C, Kuhmann S, Ketas T, Trkola A, Palani A, Clader JW, Tagat JR, et al. (2003) Analysis of the mechanism by which the small molecule CCR5 antagonists SCH-351125 and SCH-350581 inhibit human immunodeficiency virus type-1 entry. *J Virol* **77:**5201–5208.
Wu L, LaRosa G, Kassam N, Gordon CJ, Heath H, Ruffing N, Chen J, Humblias J, Samson M, Parmentier M, et al. (1997) Interaction of the chemokine receptor CCR5 with its ligands: multiple domains for HIV-1 gp120 binding and a single domain for chemokine binding. *J Exp Med* **186:**1373–1381.
Wyatt R and Sodroski J (1998) The HIV-1 envelope glycoproteins: fusogens, antigens and immunogens. *Science (Wash DC)* **280:**1884–1888.
Zhang Y-J and Moore JP (1999) Will multiple coreceptors need to be targeted by inhibitors of human immunodeficiency virus type 1 entry? *J Virol* **73:**3443–3448.

Address correspondence to: Terry Kenakin, Assay Development and Compound Profiling, GlaxoSmithKline Research and Development, 5 Moore Drive, Research Triangle Park, NC 27709. Email: Terry.P.Kenakin@gsk.com